



Large spin splitting of metallic surface-state bands at adsorbate-modified gold/silicon surfaces

SUBJECT AREAS:

ELECTRONIC PROPERTIES
AND MATERIALS

SPINTRONICS

TWO-DIMENSIONAL MATERIALS

SURFACES, INTERFACES AND
THIN FILMS

L. V. Bondarenko^{1,2}, D. V. Gruznev^{1,2}, A. A. Yakovlev¹, A. Y. Tupchaya¹, D. Usachov³, O. Vilkov³, A. Fedorov³, D. V. Vyalikh^{3,4}, S. V. Eremeev^{5,6}, E. V. Chulkov^{7,8}, A. V. Zotov^{1,2,9} & A. A. Saranin^{1,2}

Received
26 March 2013

Accepted
24 April 2013

Published
10 May 2013

Correspondence and
requests for materials
should be addressed to
A.A.S. (saranin@iacp.
dvo.ru)

¹Institute of Automation and Control Processes, 690041 Vladivostok, Russia, ²School of Natural Sciences, Far Eastern Federal University, 690950 Vladivostok, Russia, ³St. Petersburg State University, 198504 St. Petersburg, Russia, ⁴Institute of Solid State Physics, Dresden University of Technology, D-01062 Dresden, Germany, ⁵Institute of Strength Physics and Materials Science, 634021 Tomsk, Russia, ⁶Tomsk State University, 634050 Tomsk, Russia, ⁷Donostia International Physics Center (DIPC), 20018 San Sebastián/Donostia, Basque Country, Spain, ⁸Departamento de Física de Materiales and Centro Mixto CSIC-UPV/EHU, Centro de Física de Materiales CFM - Materials Physics Center MPC, Facultad de Ciencias Químicas, UPV/EHU, Apdo. 1072, 20080 San Sebastián, Basque Country, Spain, ⁹Department of Electronics, Vladivostok State University of Economics and Service, 690600 Vladivostok, Russia.

Finding appropriate systems with a large spin splitting of metallic surface-state band which can be fabricated on silicon using routine technique is an essential step in combining Rashba-effect based spintronics with silicon technology. We have found that originally poor structural and electronic properties of the Au/Si(111) $\sqrt{3} \times \sqrt{3}$ surface can be substantially improved by adsorbing small amounts of suitable species (e.g., Tl, In, Na, Cs). The resultant surfaces exhibit a highly-ordered atomic structure and spin-split metallic surface-state band with a momentum splitting of up to 0.052 Å⁻¹ and an energy splitting of up to 190 meV at the Fermi level. The family of adsorbate-modified Au/Si(111) $\sqrt{3} \times \sqrt{3}$ surfaces, on the one hand, is thought to be a fascinating playground for exploring spin-splitting effects in the metal monolayers on a semiconductor and, on the other hand, expands greatly the list of material systems prospective for spintronics applications.

Generation of spin-polarized electrons on the basis of Rashba spin splitting in the two-dimensional electron-gas systems on semiconductors is considered to be an essential step in developing semiconductor spintronics applications¹. To reach the goal, three requirements have to be satisfied as follows. First, spin splitting should be *large* enough to allow operations of the device at room temperature. Second, the surface-state band has to be *metallic* to allow significant spin transport. Third, the substrate should be a *semiconductor* as a large bulk current in metallic substrate would sweep off the surface spin signal. In addition, due to device application reasons it is highly desirable that the substrate would be a *silicon*, the most widely used semiconductor material. The last demand is that the structure could be easily fabricated using *routine technique*, e.g., molecular beam epitaxy.

The last decade has been marked by the step-by-step progress in this direction. The surface Rashba effect was first found on the metal surfaces like Au(111)^{2,3} and Bi(111)^{4,5} and a giant spin splitting was detected on Bi-covered Ag(111)^{6,7}. The latter finding indicates that a large spin splitting is possible (and even enhances) when only a monolayer of a heavy element is placed on a surface of a light element. This discovery stimulated expanding the search area to semiconductor surfaces such as Si and Ge covered by heavy-metal monolayers. Large Rashba splitting has been found on Bi/Si(111)⁸⁻¹⁰, Bi/Ge(111)¹¹, Tl/Si(111)^{12,13}, and Pt/Si(110)¹⁴ surfaces but it occurs in the *non-metallic* surface-state bands. The first metal/semiconductor reconstruction with a spin splitting of *metallic* surface-state band found was the Pb/Ge(111) $\sqrt{3} \times \sqrt{3}$ ^{15,16} followed by the Au/Ge(111) $\sqrt{3} \times \sqrt{3}$ ¹⁷⁻¹⁹. As indicated in Ref. 15, the spin-splitting effect does not depend on any peculiar property of Ge, hence it seems possible to realize a similar electronic structure on a Si surface. In this respect, the Au/Si(111) $\sqrt{3} \times \sqrt{3}$ reconstruction is thought to be a promising candidate as its atomic arrangement (described by the conjugated



honeycomb chained-trimer (CHCT) model^{20,21} (see Fig. 1e) is similar to that of the Au/Ge(111) $\sqrt{3} \times \sqrt{3}$ ^{22,23} and a strong Rashba-type spin-orbit splitting in it has already been predicted theoretically²¹. Substantial Rashba effect observed for self-assembled Au nanowires on vicinal Si surfaces^{24,25} also supports the suggested prospects of the Au/Si material systems. However, the structural and electronic properties of Au/Si(111) $\sqrt{3} \times \sqrt{3}$ surface are actually poor due to a presence of random domain walls. Fortunately, the breakthrough way was found to improve the surface, namely, adding small amount of In eliminates completely domain walls²⁶ and enhances metallic surface band filling²⁷. It has been recognized that after the transformation the basic CHCT structure of the original Au/Si(111) $\sqrt{3} \times \sqrt{3}$ surface is preserved, while the indium adsorbate forms a 2D gas of adatoms on it^{21,26,27}.

In the present study, we have revealed that the above effect is not a peculiar feature of only In, but is a common trait for a set of adsorbate species (e.g., Na, Cs, and Tl). Scanning tunneling microscopy (STM) and low-energy electron diffraction (LEED) observations have shown that adsorption of each above mentioned species onto the Au/Si(111) $\sqrt{3} \times \sqrt{3}$ produces a homogeneous well-ordered surface. In addition, angle-resolved photoelectron spectroscopy (ARPES) and spin-resolved ARPES data as well as first-principles calculations clearly demonstrate occurrence of the well-defined metallic surface-state band with a large spin splitting. Thus, finding such a family of adsorbate-modified Au/Si(111) systems (having the same $\sqrt{3} \times \sqrt{3}$ reconstruction) paves a way to combine Rashba-effect based spintronics with a silicon technology.

Results

Figure 1a illustrates structural and electronic properties of the pristine Au/Si(111) $\sqrt{3} \times \sqrt{3}$ surfaces. One can see that the main characteristic structural feature of the surface is a disordered meandering domain-wall network²⁸. Such a surface displays the $\sqrt{3} \times \sqrt{3}$ LEED pattern with cloudlike diffraction streaks in between $\sqrt{3}$ spots^{27,29}. As for its electronic properties, the surface is known to be metallic²⁹, but its metallicity is not strongly expressed: the surface-state spectral

features are smeared due to the domain walls and electron filling of the metallic S_1 surface band is rather low, ~ 0.1 electrons per unit cell²⁷. In the ARPES spectra, the S_1 band is invisible in the first surface Brillouin zone (SBZ) (Fig. 1a) and its faint traces can be detected only in the higher SBZs²⁷.

Adding 0.15 ± 0.05 ML of Tl, In, Na or Cs atoms to this surface produces strong effect on its structure, namely, the domain walls disappear and homogeneous well-ordered surface forms (Fig. 1b–d, upper panel). Consequently, a sharp $\sqrt{3} \times \sqrt{3}$ LEED pattern without any other features develops (not shown). STM observations reveal that the adsorbed species are present at the surface as adatoms which are mobile at room temperature but can be frozen at fixed positions by cooling the sample down to ~ 100 K (except for Cs atoms which motion is frozen only at ~ 30 K).

ARPES observations demonstrate that upon adding adsorbates (Fig. 1b–d, lower panel) all spectral features of the initial Au/Si(111) $\sqrt{3} \times \sqrt{3}$ surface are preserved but become noticeably sharp due to removal of domain walls. All bands are shifted down towards the higher binding energy and the well-defined metallic S_1 surface state band develops (being clearly seen even in the first SBZ). Electron filling of the S_1 band increases three to seven times (up to ~ 0.3 – 0.7 electrons per unit cell). Next important feature is that the metallic S_1 surface state is split. The splitting being modest along the $\bar{\Gamma}$ - \bar{K} direction becomes substantial along the $\bar{\Gamma}$ - \bar{M} direction (Fig. 2a). To reveal a spin-split character of the metallic surface states, we have performed the spin-resolved ARPES measurement on Tl-adsorbed system. Figure 2b shows the spin-resolved energy distribution curves of S_1^A and S_1^B subbands at $k_{\parallel} = 0.30 \text{ \AA}^{-1}$ (here and below we refer inner and outer subbands as S_1^A and S_1^B , respectively). This result clearly shows that the S_1 state is spin-split and the spin orientations are opposite in A and B subbands.

Figure 3 summarizes the results for various adsorbate species. All spectra have a qualitatively similar appearance but the splitting value varies. Momentum splitting at the Fermi level Δk_{\parallel} ranges from $\sim 0.018 \text{ \AA}^{-1}$ obtained for Cs to that of $\sim 0.052 \text{ \AA}^{-1}$ for Tl. Consequently, energy splitting ΔE_F changes in the range from

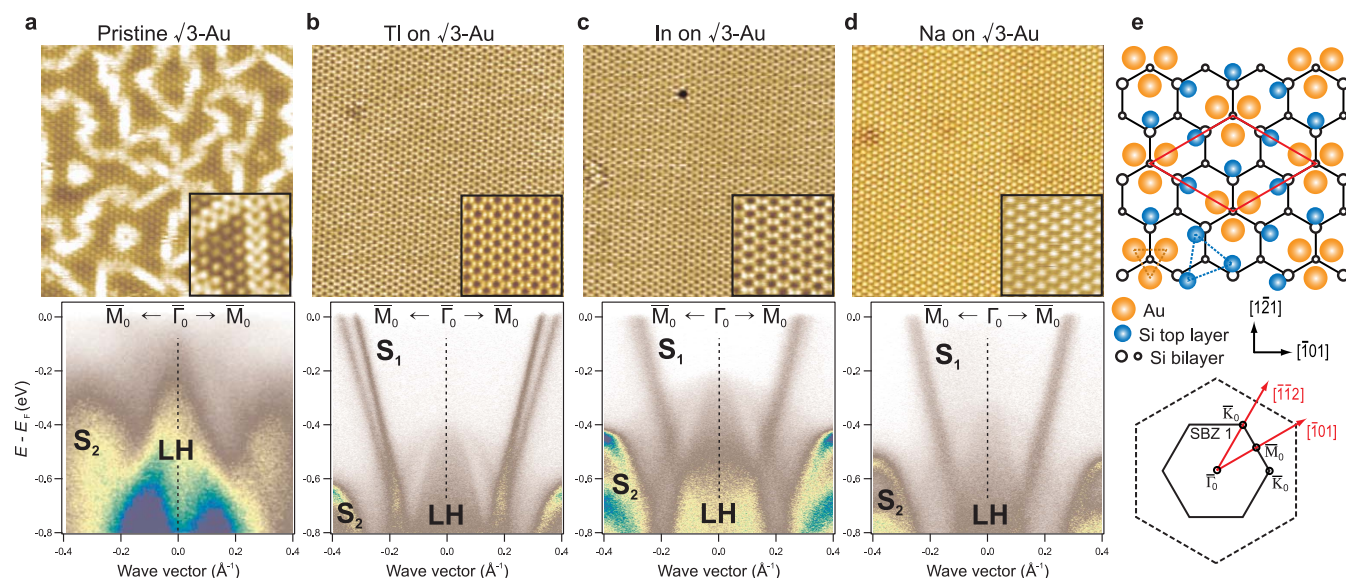


Figure 1 | Adsorbate-induced transformations in structural and electronic properties of Au/Si(111). STM images and ARPES spectra taken in the first $\sqrt{3} \times \sqrt{3}$ surface Brillouin zone (SBZ) along the \bar{M} - $\bar{\Gamma}$ - \bar{M} direction from (a) pristine Au/Si(111) $\sqrt{3} \times \sqrt{3}$ surface and the same surface after adsorption of 0.15 ± 0.05 ML of (b) Tl, (c) In, and (d) Na. Scale of the STM images is $250 \times 250 \text{ \AA}^2$, that of the insets is $50 \times 50 \text{ \AA}^2$. Note that ARPES data are confined to the interior of SBZ as exact position of the \bar{M} point is at 0.546 \AA^{-1} . (e) Atomic arrangement (CHCT model) of the Au/Si(111) $\sqrt{3} \times \sqrt{3}$ surface consisting of Au trimers (shown by orange circles) and Si trimers (shown by blue circles) residing on Si(111) bilayer (shown by black circles) and sketch of reciprocal space geometry with boundaries of the first $\sqrt{3} \times \sqrt{3}$ SBZ given by black lines (dashed hexagon depicts the 1×1 SBZ). The high symmetry points are marked by circles.

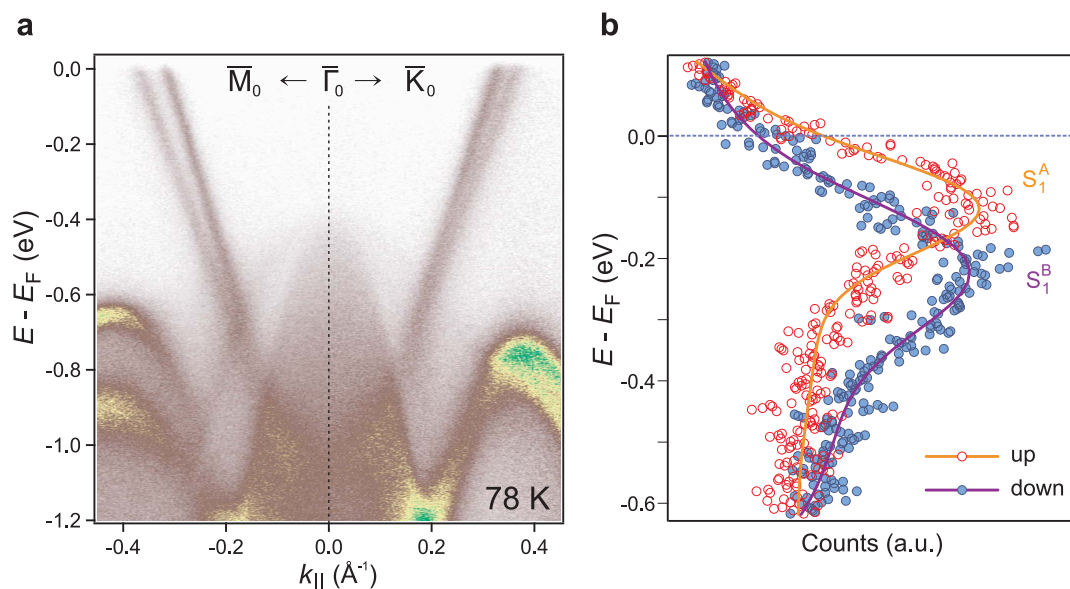


Figure 2 | Splitting of dispersion curves measured by ARPES and spin-resolved ARPES. (a) Band structure along the $\bar{M}-\bar{\Gamma}-\bar{K}$ of the Tl-adsorbed Au/Si(111) $\sqrt{3} \times \sqrt{3}$ surface determined with spin-unpolarized ARPES. Data are confined to the interior of SBZ as exact positions of the \bar{M} and \bar{K} points are at 0.546 \AA^{-1} and 0.630 \AA^{-1} , respectively. (b) Spin-resolved ARPES spectra taken for the same surface at a fixed $k_{\parallel} = 0.30 \text{ \AA}^{-1}$ in the $\bar{\Gamma}-\bar{M}$ direction.

$\sim 100 \text{ meV}$ to $\sim 190 \text{ meV}$. From the graph shown in Fig. 3b one can conclude that the splitting value is essentially controlled by position of the Fermi level, i.e., by the electron filling of the S_1 band. The concept is illustrated in Fig. 3c where the experimental dots from Fig. 3b are superposed on the S_1^A and S_1^B dispersion curves of the calculated band structure. One can see that by choosing appropriate adsorbate species the Fermi level position can be tuned within the range of $\sim 350 \text{ meV}$ (shown by the pink shaded area in Fig. 3c). Position of Fermi level also varies slightly depending on concentration of a given adsorbate.

Figure 4a shows the ARPES Fermi surface of the Tl-adsorbed Au/Si(111) $\sqrt{3} \times \sqrt{3}$. One can clearly see the two Fermi contours of which the outer (corresponding to the S_1^B band) has an almost

circular shape while the inner (corresponding to the S_1^A band) has a shape of a smoothed hexagon. As the hexagon corners lies at the $\bar{\Gamma}-\bar{K}$ directions, these are the directions of the minimal splitting, while the greatest splitting is at the hexagon sides (i.e., along the $\bar{\Gamma}-\bar{M}$ directions). One can see that the calculated constant energy contours (Fig. 4b) properly reproduce all the principal features of the experimentally derived Fermi surface map. The only small deviation that can be noticed is the discrepancy between the calculated and experimental splitting along the $\bar{\Gamma}-\bar{K}$ direction where theory yields slightly underestimated value (Fig. 4c).

Figure 4b also shows the clockwise and counterclockwise spin helicity for the inner and outer contours, respectively, with abrupt change of the sign for out-of-plane spin component at the $\bar{\Gamma}-\bar{K}$

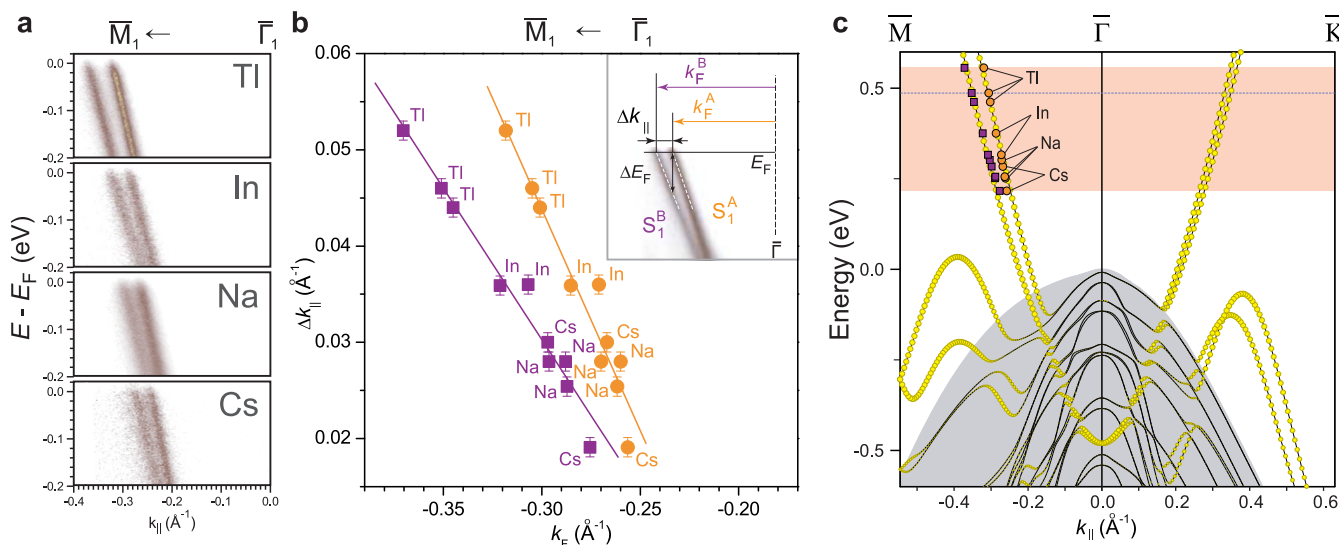


Figure 3 | Effect of adsorbate species. (a) Fragments of the ARPES spectra taken in the $\bar{\Gamma}-\bar{M}$ direction near the Fermi level of the Tl-, In-, Na-, and Cs-adsorbed Au/Si(111) $\sqrt{3} \times \sqrt{3}$ surfaces. (b) Momentum splitting at the Fermi level Δk_{\parallel} plotted as a function of the Fermi wave vector k_F for S_1^A and S_1^B bands measured for various species (as indicated in the graph). (c) Calculated band structure along the $\bar{M}-\bar{\Gamma}-\bar{K}$ with the experimental dots from (b) superposed on the S_1^A and S_1^B dispersion curves. Surface state bands are shown by filled yellow circles, shaded region indicates projected bulk bands. Range of the varied Fermi level position is indicated by the pink shaded area.

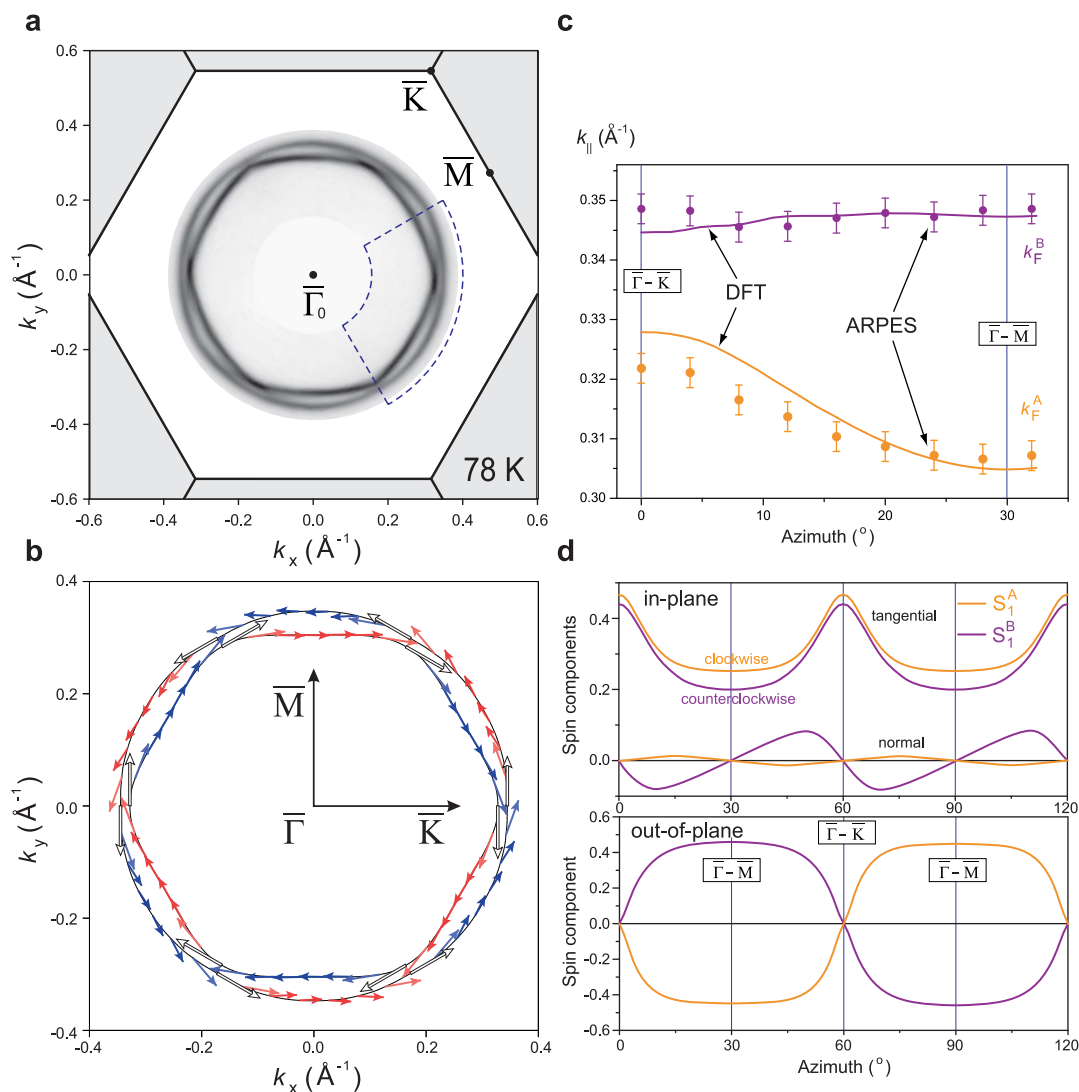


Figure 4 | Fermi surface and spin texture. (a) Symmetrized Fermi surface of the TI-adsorbed Au/Si(111) $\sqrt{3} \times \sqrt{3}$ surface determined with ARPES. The k -space area where the ARPES measurements were carried out is outlined by a dashed blue line. (b) Constant energy contours at energy marked by dashed blue line in Fig. 3c. Arrows along the contours and their length indicate the in-plane spin component. The out-of-plane spin component is indicated by the colour with red and blue corresponding to the upward and downward directions, respectively. White colour indicates fully in-plane spin alignment. (c) Azimuthal dependence of the Fermi wave vector k_F for the S_1^A and S_1^B bands. Experimental and calculated data are presented by dots and solid lines, respectively. (d) Azimuthal dependencies of the spin components, including in-plane components in the directions tangential and normal to the Fermi contour (upper panel) and out-of-plane component (lower panel).

directions, which is intrinsic feature of the Rashba-split surface states at hexagonal surfaces¹². The detailed spin texture is illustrated in Fig. 4d. Figure 4d (upper panel) shows the azimuthal dependencies of in-plane components in the tangential and normal directions to the S_1^A and S_1^B Fermi contours. One can see that tangential components for both bands demonstrate a very similar behavior with sharp maxima in the $\bar{\Gamma}$ - \bar{K} directions and wide minima around the $\bar{\Gamma}$ - \bar{M} directions. The normal component (a signature of the Dresselhaus term) is small for the inner S_1^A band but it becomes noticeable for the outer S_1^B band and demonstrates an undulating behavior. Maximal deviation of the in-plane spin component from a purely tangential is $\sim 3^\circ$ and $\sim 16^\circ$ for the S_1^A and S_1^B subbands, respectively. For both bands, the out-of-plane z component (Fig. 4d, lower panel) remains almost constant in the wide area near the $\bar{\Gamma}$ - \bar{M} directions and abruptly changes its sign going through zero while crossing the $\bar{\Gamma}$ - \bar{K} directions. As a result, spin has a fully in-plane alignment there. The calculations have also revealed that changing the Fermi level position affects the spin texture of the S_1 band. Upon the downward

shift of the Fermi level from its highest position, corresponding to TI-adsorbed surface to its lowest position obtained on Cs-modified Au/Si(111) surface (see pink stripe in Fig. 3c) the maximal deviation of the in-plane spin component from a purely tangential increases up to $\sim 24^\circ$ for the S_1^B subband while that for the S_1^A subband remains $\sim 3^\circ$. At the same time this shift of the Fermi level leads to decreasing maximal out-of-plane spin tilt angle from $\sim 68(63)^\circ$ to $\sim 64(53)^\circ$ for the outer(inner) subband.

Discussion

Our results show that chemically very different species, alkali metals, Na and Cs, and heavy group-III metals, In and Tl, when being adsorbed onto the Au/Si(111) $\sqrt{3} \times \sqrt{3}$ surface, affect its structural and electronic properties in a very similar way, namely, eliminate domain walls and donate electrons to the metallic S_1 surface state band. DFT calculations for In-adsorbed surface²⁶ showed that removal of domain walls is due to a stress-relieving effect produced by In adsorption. However, origin of this effect was not disclosed.



Typically, surface lattice stress changes when foreign atoms become incorporated directly into the lattice and the greater the size difference between the host and foreign atoms the greater the stress. This typical scenario is apparently not held for the present case where foreign adatoms are not incorporated into the lattice and their atomic size does not play a decisive role. As an alternative, we suggest that adsorbates can affect the surface lattice stress by donating electrons to the substrate surface layer. As a result, the top layer possesses a non-compensated charge which means adding a Coulomb repulsion term into the interactions between surface atoms, hence changing the surface stress.

We have found a number of adsorbate species (Tl, In, Na, and Cs) which make the Au/Si(111) $\sqrt{3} \times \sqrt{3}$ surface suitable for observing significant spin-orbit splitting. We believe that the list of such adsorbates can be extended (at least, at the expense of the left alkali metals). The main requirements for candidate species seem to be as follows. First, they are metals that could easily donate a sufficient amount of electrons to the surface state band. This could be attained with species like monovalent alkali metals with high electropositivity and/or species having several valent electrons, as Group-III metals. In this respect, it is worth noting the very recent finding that extra Au or Ge atoms produce a similar doping effect on Au/Ge(111) $\sqrt{3} \times \sqrt{3}$ surface³⁰, thus extending further the list of possible candidate species. Second, they have to preserve the original Au trimer structure (which is believed to be responsible for the spin-splitting effect¹⁸) or, in other words, they should not form 2D alloys with Au on Si(111) surface. For example, in contrast to In and Tl, the other group-III metals, Al and Ga, are not suitable, as they form binary reconstructions with Au, (Au,Al)/Si(111) $3\sqrt{3} \times 3\sqrt{3}$ ³¹, (Au,Al)/Si(111) 2×2 ³¹, and (Au,Ga)/Si(111) $3\sqrt{3} \times 3\sqrt{3}$.

As the list is open, many species are expected to produce a similar effect on the structure and electronic properties of the Au/Si(111) $\sqrt{3} \times \sqrt{3}$ surface. However, similarity does not mean identity, that makes the family of adsorbate-modified Au/Si(111) $\sqrt{3} \times \sqrt{3}$ reconstructions to be a promising playground for exploring spin-splitting effects as a function of structural parameters tuned by adsorption of particular species. On the other hand, they represent a wide set of surface systems for the choice of the proper ones for spintronic device applications.

Another degree of freedom for tailoring electronic properties stems from ability to intermix Si and Ge into a desired Si_xGe_{1-x} alloy layer. Though Si and Ge are akin elements and their $\sqrt{3} \times \sqrt{3}$ -Au reconstructions have the same atomic arrangement, their electronic structures exhibit essential differences. While the Au/Si(111) $\sqrt{3} \times \sqrt{3}$ surface has a single metallic S₁ band, the Au/Ge(111) $\sqrt{3} \times \sqrt{3}$ surface in addition to the electronic S₁ band has the hole bands dispersing up to the Fermi level^{17,18}. The spin textures of the S₁ bands for these surfaces are similar but also not identical, namely, contribution of the Dresselhaus terms for the Au/Ge(111) $\sqrt{3} \times \sqrt{3}$ is substantially greater¹⁹. Thus, the variable Au/Si_xGe_{1-x}(111) $\sqrt{3} \times \sqrt{3}$ surfaces might be a new interesting object for exploring spin-splitting effects in metal monolayers on semiconductor.

Methods

Sample preparation method. The STM and ARPES experiments were performed in an ultra-high-vacuum system with a base pressure of $\sim 2.0 \times 10^{-10}$ Torr. Atomically-clean Si(111) 7×7 surfaces were prepared *in situ* by flashing to 1280°C after the samples were first outgassed at 600°C for several hours. Pristine Au/Si(111) $\sqrt{3} \times \sqrt{3}$ surfaces were formed by Au deposition onto Si(111) 7×7 surface held at $\sim 600^\circ\text{C}$. The adsorbate-modified Au/Si(111) surfaces were prepared by adsorbing 0.15 \pm 0.05 ML of a given species, In, Na or Cs, onto the surface held at $\sim 350^\circ\text{C}$. Due to significant desorption, deposition of Tl was performed at room temperature followed by annealing at $\sim 350^\circ\text{C}$. Adsorbate deposition was terminated when STM shows domain-wall-free surface and LEED displays a sharp $\sqrt{3} \times \sqrt{3}$ pattern without any other features.

STM. STM images were acquired using Omicron variable-temperature STM-XA operating in a constant-current mode. Electrochemically-etched W tips and mechanically cut PtIr tips were used as STM probes after annealing in vacuum.

ARPES and spin-resolved ARPES. ARPES measurements were conducted in the ultrahigh vacuum chamber Omicron MULTIPROBE using VG Scienta R3000 electron analyzer and high-flux He discharge lamp ($h\nu = 21.2$ eV) with toroidal-grating monochromator as a light source. Spin-resolved ARPES and part of ARPES measurements were performed at the novel SR-ARPES facility of RGL at BESSY, U125-2, SGM beamline using VG Scienta R4000 analyzer with Mott detector operating at 25 keV.

First-principles calculations. Our calculations were based on DFT as implemented in the Vienna *ab initio* simulation package VASP^{32,33}, using a planewave basis and the projector augmented-wave approach³⁴ for describing the electron-ion interaction. The generalized gradient approximation (GGA) of Perdew, Burke, and Ernzerhof (PBE)³⁵ has been used for the exchange correlation (XC) potential. The Hamiltonian contains the scalar relativistic corrections, and the spin-orbit interaction (SOI) was taken into account by the second variation method as has been implemented in VASP by Kresse and Lebacz³⁶. To simulate the $\sqrt{3} \times \sqrt{3}$ -CHCT reconstruction we use a slab consisting of 12 bilayers. Hydrogen atoms were used to passivate the Si dangling bonds at the bottom of the slab. Both bulk Si lattice constant and the atomic positions within the three topmost bilayers of the slab were optimized including SOI self-consistently. The silicon atoms of deeper layers were kept fixed at the bulk crystalline positions.

- Sinova, J. *et al.* Universal intrinsic spin Hall effect. *Phys. Rev. Lett.* **92**, 126603 (2004).
- LaShell, S., McDougall, B. A. & Jensen, E. Spin splitting of an Au(111) surface state band observed with angle resolved photoelectron spectroscopy. *Phys. Rev. Lett.* **77**, 3419–3422 (1996).
- Hoesch, M. *et al.* Spin structure of the Shockley surface state on Au(111). *Phys. Rev. B* **69**, 241401 (2004).
- Koroteev, Y. M. *et al.* Strong spin-orbit splitting on Bi surfaces. *Phys. Rev. Lett.* **93**, 046403 (2004).
- Kimura, A. *et al.* Strong Rashba-type spin polarization of the photocurrent from bulk continuum states: Experiment and theory for Bi(111). *Phys. Rev. Lett.* **105**, 076804 (2010).
- Ast, C. R. *et al.* Giant spin splitting through surface alloying. *Phys. Rev. Lett.* **98**, 186807 (2007).
- Bihlmayer, G., Blügel, S. & Chulkov, E. V. Enhanced Rashba spin-orbit splitting in Bi/Ag(111) and Pb/Ag(111) surface alloys from first principles. *Phys. Rev. B* **75**, 195414 (2007).
- Gierz, I. *et al.* Silicon surface with giant spin splitting. *Phys. Rev. Lett.* **103** (4), 046803–4 (2009).
- Sakamoto, K. *et al.* Peculiar Rashba splitting originating from the two-dimensional symmetry of the surface. *Phys. Rev. Lett.* **103** (15), 156801–4 (2009).
- Frantzeskakis, E., Pons, S. & Grioni, M. Band structure scenario for the giant spin-orbit splitting observed at the Bi/Si(111) interface. *Phys. Rev. B* **82** (8), 085440–11 (2010).
- Ohtsubo, Y. *et al.* Spin-polarized semiconductor surface states localized in subsurface layers. *Phys. Rev. B* **82** (20), 201307–4 (2010).
- Sakamoto, K. *et al.* Abrupt rotation of the Rashba spin to the direction perpendicular to the surface. *Phys. Rev. Lett.* **102** (9), 096805–4 (2009).
- Ibañez-Azpiroz, J., Eiguren, A. & Bergara, A. Relativistic effects and fully spin-polarized Fermi surface at the Tl/Si(111) surface. *Phys. Rev. B* **84** (12), 125435–6 (2011).
- Park, J. *et al.* Self-assembled nanowires with giant Rashba split band. *Phys. Rev. Lett.* **110** (3), 036801–5 (2013).
- Yaji, K. *et al.* Large Rashba spin splitting of a metallic surface-state band on a semiconductor surface. *Nature Commun.* **1**, 17–5 (2010).
- Yaji, K., Hatta, S., Aruga, T. & Okuyama, H. Structural and electronic properties of the Pb/Ge(111)- $\beta(\sqrt{3} \times \sqrt{3})$ R30° surface studied by PES and first-principles calculations. *Phys. Rev. B* **86** (23), 235317–6 (2012).
- Höpfner, P. *et al.* Electronic band structure of the two-dimensional metallic electron system Au/Ge(111). *Phys. Rev. B* **83** (23), 235435–8 (2011).
- Nakatsuji, K. *et al.* Anisotropic splitting and spin polarization of metallic bands due to spin-orbit interaction at the Ge(111)($\sqrt{3} \times \sqrt{3}$)R30°-Au surface. *Phys. Rev. B* **84** (3), 035436–4 (2011).
- Höpfner, P. *et al.* Three-dimensional spin rotations at the Fermi surface of a strongly spin-orbit coupled surface system. *Phys. Rev. Lett.* **108** (18), 186801–5 (2012).
- Ding, Y. G., Chan, C. T. & Ho, K. M. Theoretical investigation of the structure of the ($\sqrt{3} \times \sqrt{3}$)R30°-Au/Si(111) surface. *Surf. Sci.* **275** (3), L691–L696 (1992).
- Hsu, C. H., Lin, W. H., Ozolins, V. & Chuang, F. C. Electronic structure of the indium-adsorbed Au/Si(111)- $\sqrt{3} \times \sqrt{3}$ surface: A first-principles study. *Phys. Rev. B* **85** (15), 155401–7 (2012).
- Howes, P. B., Norris, C., Finney, M. S., Vlieg, E. & van Silfhout, R. G. Structure of Ge(111) $\sqrt{3} \times \sqrt{3}$ -Au determined by surface X-ray-diffraction. *Phys. Rev. B* **48** (3), 1632–1642 (1993).
- Over, H., Wang, C. P. & Jona, F. Atomic bond configuration of Ge(111)-($\sqrt{3} \times \sqrt{3}$)R30°-Au: A low-energy electron-diffraction study. *Phys. Rev. B* **51** (7), 4231–4235 (1995).



24. Barke, I., Zheng, F., Rügheimer, T. K. & Himpsel, F. J. Experimental evidence for spin-split bands in a one-dimensional chain structure. *Phys. Rev. Lett.* **97** (22), 226405–4 (2006).
25. Okuda, T. *et al.* Large out-of-plane spin polarization in a spin-splitting one-dimensional metallic surface state on Si(557)-Au. *Phys. Rev. B* **82** (16), 161410–4 (2010).
26. Gruznev, D. V. *et al.* Si(111)- $\alpha\sqrt{3} \times \sqrt{3}$ -Au phase modified by In adsorption: Stabilization of a homogeneous surface by stress relief. *Phys. Rev. B* **73** (11), 115335–7 (2006).
27. Kim, J. K. *et al.* Two-dimensional electron gas formed on the indium-adsorbed Si(111) $\sqrt{3} \times \sqrt{3}$ -Au surface. *Phys. Rev. B* **80** (7), 075312–7 (2009).
28. Nagao, T. *et al.* Structural phase transitions of Si(111)-($\sqrt{3} \times \sqrt{3}$)R30°-Au: Phase transitions in domain-wall configurations. *Phys. Rev. B* **57** (16), 10100–10109 (1998).
29. Zhang, H. M., Balasubramanian, T. & Uhrberg, R. I. G. Surface electronic structure study of Au/Si(111) reconstruction: Observation of crystal-to-glass transition. *Phys. Rev. B* **66** (16), 165402–6 (2002).
30. Nakatsujii, K., Motomura, Y., Niikura, R. & Komori, F. Selective doping in a surface band and atomic structures of the Ge(111)($\sqrt{3} \times \sqrt{3}$)R30°-Au surface. *J. Phys.:Cond. Matt.* **25** (4), 045007–9 (2013).
31. Khrantsova, E. A., Saranin, A. A., Chub, A. B. & Lifshits, V. G. Al and Au binary surface phases on the Si(111) surface. *Surf. Sci.* **331/333** (1), 594–599 (1995).
32. Kresse, G. & Hafner, J. *Ab initio* molecular dynamics for liquid metals. *Phys. Rev. B* **47**, 558 (1993).
33. Kresse, G. & Joubert, D. From ultrasoft pseudopotentials to the projector augmented-wave method. *Phys. Rev. B* **59**, 1758 (1999).
34. Blöchl, P. E. Projector augmented-wave method. *Phys. Rev. B* **50**, 17953–17979 (1994).
35. Perdew, J. P., Burke, K. & Ernzerhof, M. Generalized gradient approximation made simple. *Phys. Rev. Lett.* **77**, 3865–3868 (1996).
36. Kresse, G. & Lebacqz, O. The VASP manual. [http://cms.mpi.univie.ac.at/vasp/vasp.html](http://cms.mpi.univie.ac.at/vasp/vasp/vasp.html). Retrieved April 22, 2013.

Acknowledgements

Part of this work was supported by the Russian Foundation for Basic Research (Grant Nos. 11-02-98515r, 12-02-00416, 12-02-00430 and 12-02-31745), the Ministry of Education and Science of the RF (Grant Nos. 8022, 8581, 2.8575.2013 and 2.1004.2011), NSH-774.2012.2, the Basque Country Government, Departamento de Educación, Universidades e Investigación (Grant No. IT-366-07), the Spanish Ministerio de Ciencia e Innovación (Grant No. FIS2010-19609-C02-00), German-Russian Interdisciplinary Science Center (G-RISC) funded by the German Federal Foreign Office via the German Academic Exchange Service (DAAD) and Helmholtz Zentrum Berlin für Materialien und Energie for support within a bilateral Program “Russian-German Laboratory” at BESSY-II. We thank S.S. Tsirkin for help with graphical presentation of results. D.U. and A.F. acknowledge support from SPbU grant.

Author contributions

D.V.G. and L.V.B. carried out ARPES and STM under the support of A.A.Y. and A.Y.T. L.V.B., D.U., O.V. and A.F. carried out ARPES and spin-resolved ARPES at BESSY-II with guidance from D.V.V. S.V.E. and E.V.C. carried out the theoretical calculation. D.V.G., A.V.Z. and A.A.S. analyzed the data and wrote the manuscript with input from S.V.E. and E.V.C. and conceived and coordinated the project.

Additional information

Competing financial interests: The authors declare no competing financial interests.

License: This work is licensed under a Creative Commons Attribution-NonCommercial-NoDerivs 3.0 Unported License. To view a copy of this license, visit <http://creativecommons.org/licenses/by-nc-nd/3.0/>

How to cite this article: Bondarenko, L.V. *et al.* Large spin splitting of metallic surface-state bands at adsorbate-modified gold/silicon surfaces. *Sci. Rep.* **3**, 1826; DOI:10.1038/srep01826 (2013).